RESEARCH ARTICLE | JULY 23 2008

Evidence for tunneling in reverse-biased III-V photodetector diodes

S. R. Forrest; M. DiDomenico, Jr.; R. G. Smith; ... et. al

Appl. Phys. Lett. 36, 580–582 (1980)
https://doi.org/10.1063/1.91553

Evidence for tunneling in reverse-biased III-V photodetector diodes

S. R. Forrest, M. DiDomenico, Jr., R. G. Smith, and H. J. Stocker
Bell Laboratories, Murray Hill, New Jersey 07974

(Received 25 October 1979; accepted for publication 14 January 1980)

Photodiodes made from III-V group semiconductor alloys have been found to exhibit anomalously high dark currents. We present evidence that tunneling is the dominant source of dark current in many cases. The tunneling current becomes substantial at peak junction electric fields as low as 10^5 V/cm due to the small direct energy gaps and small effective masses of the materials tested. Tunneling sets limits on the magnitude of the electric field attainable in these materials, and therefore has serious implications on photodetector design and performance.

PACS numbers: 72.80.Ey, 79.70. + q, 72.20.Ht

Photodiodes made from group III-V semiconductor alloys are under investigation for use as optical detectors in long wavelength (1.2 to 1.6 μm) light wave communication systems. In many cases, these diodes exhibit anomalously high dark currents,[1-5] which limit their ultimate sensitivity as photodetectors.[6] The current is found to increase nearly exponentially with applied voltage — a behavior uncharacteristic of either generation-recombination or diffusion leakage currents. In this letter we present evidence that, in many cases, the tunneling of electrons into the conduction band is a significant source of reverse-biased diode leakage current. The observed dependence of current on temperature and applied voltage is shown to be consistent with the tunneling model.

Band-to-band tunneling current in reverse-biased, direct gap semiconductors is given by[7]:

$$I = \frac{(2m^*)^{1/2}q^3EVA}{4\pi^2\hbar^2\epsilon_g^{1/2}} \exp\left(-\frac{\theta m_0^{1/2}\epsilon_g^{3/2}}{q\hbar E}\right). \quad (1)$$

Here, m^* is the effective mass of the tunneling carrier, m_0 is the free electron mass, E the electric field, V the applied voltage across the junction, A the junction area, ϵ_g the direct band gap, and q the electronic charge. The parameter θ is a dimensionless quantity given by

$$\theta = \alpha(m^*/m_0)^{1/2}, \quad (2)$$

where α is a constant on the order of unity, characteristic of the barrier shape. The exponential term in Eq. (1) is the probability that a carrier in the valence band will tunnel into the conduction band. The prefactor to the exponential depends on the density and occupancy of states in both the valence and conduction bands. Equation (1) is valid when $|V + V_{bi}| \geqslant \epsilon_g/q$, where V_{bi} is the built-in potential of the junction. Note that the tunneling current is strongly dependent on the ratio $\epsilon_g^{3/2}/E$; therefore, this mechanism can account for the nearly exponential dependence of dark current on applied voltage.

To determine if tunneling is a significant contributor to the reverse leakage current in several III-V semiconductor diodes, we have investigated the dependence of reverse-biased leakage current on both ϵ_g and E and compared our results[8] with Eq. (1). A summary of relevant parameters for the diodes tested is given in the first six columns of Table I. Samples A, B, and C are etched-mesa diodes; A and B consist of a layer of $In_xGa_{1-x}As_yP_{1-y}$ grown via liquid-phase epitaxy on an InP substrate, while C is an InP sample. Samples D, E, and F are planar devices consisting of a layer of $Ga_xAl_{1-x}As$ grown via liquid-phase epitaxy on a GaAs substrate. Only diodes apparently free of microplasmas (as evidenced by smooth I-V characteristics) and free of abnormally high noise current were selected for measurement.

TABLE I. Summary of device parameters.

Sample	Material	ϵ_g at 300 K (eV)	$\bar{N}$[a] (cm^{-3})	E_m[b] $\times 10^{-5}$ (V/cm)	$\epsilon_g^{3/2}/E_m \times 10^5$ ($eV^{3/2}$ cm/V)	θ	m^*/m_0[c]
A	$In_{0.74}Ga_{0.26}As_{0.56}P_{0.44}$	1.03	2.1×10^{16}	1.7 ± 0.2	0.62	0.23 ± 0.03	0.04
B	$In_{0.74}Ga_{0.26}As_{0.56}P_{0.44}$	1.04	1.1×10^{16}	0.80 ± 0.08	1.3	0.11 ± 0.02[d]	0.01
C	InP	1.35	2.7×10^{17}	5.2 ± 0.5	0.30	0.19 ± 0.03	0.03
				3.2 ± 0.3	0.49	0.15 ± 0.02	0.02
				1.6 ± 0.2	0.98	0.14 ± 0.03	0.02
D	$Ga_{0.90}Al_{0.10}As$	1.48	3.7×10^{17}	7.8 ± 0.8	0.23	0.15 ± 0.02	0.02
E	$Ga_{0.85}Al_{0.15}As$	1.51	6.3×10^{17}	6.1 ± 0.6	0.30	0.16 ± 0.02	0.02
F	$Ga_{0.90}Al_{0.10}As$	1.46	1.1×10^{16}	2.4 ± 0.2	0.74	...	...
				0.6 ± 0.1	2.9	...	...

[a] $\bar{N} = (x_m - x_0)^{-1}\int_{x_0}^{x_m} N(x)dx$, where x_m, x_0 = depletion region width at $I \simeq 10\,\mu$A and $I = 0$, respectively.
[b] E_m is maximum field at bias where $\log(I)$-vs-$\epsilon_g^{3/2}$ data, as presented in Fig. 1, were measured.
[c] Assumes parabolic barrier potential.
[d] Fit to linear region of data only.

 0003-6951/80/070580-03$00.50

Also, the I-V characteristics were reproducible after thermally cycling the devices.

In Fig. 1, $\log(I)$ at fixed voltage is plotted versus $\epsilon_g^{3/2}$ for the diodes listed in Table I. The band gap, as determined from reverse-biased diode photoresponse, was varied by approximately 10% by varying junction temperature from 77 to 420 K. Since carrier concentration varies only weakly with temperature for these samples, constant voltage implies constant electric field[9] over the entire temperature range considered. With the exception of the low-doped samples B and F (where the electric field, and hence the tunneling currents, are small), the $\log(I)$-vs-$\epsilon_g^{3/2}$ data are linear as predicted by Eq. (1). The lines in the figure represent best fits of the data to the form $I = \beta \exp(-\gamma\epsilon_g^{3/2})$. The parameter θ is obtained from the fitting parameter γ and the junction electric field. The field is obtained from the junction doping profile calculated from capacitance-vs-voltage measurements of the diode. In determining θ, only the maximum value of electric field E_m is used, since tunneling current decreases rapidly with decreasing field.

Values of θ for the data in Fig. 1 are listed in Table I. The main source of uncertainty in θ results from systematic errors ($\sim 10\%$) in the measurement of E_m. We find θ is between 0.14 and 0.23 for all samples whose leakage current follows Eq. (1). If we assume the gap potential barrier is parabolic, then[7] $\alpha = \pi/(2\sqrt{2})$ [see Eq. (2)]. In Table I we give the effective mass obtained for a parabolic barrier using the measured values of θ. Discrepancies between measurement and $0.04 \leqslant m^*/m_0 \leqslant 0.06$ expected for these materials[10] may be due to the value of α used. In choosing α, we have ignored more complicated potential barrier shapes, variations in ϵ_g across the junction due to varying composition of the epitaxial layers, and variations in E_m across the junction area. The agreement between the accepted values of effective mass and those inferred from the present measurements is reasonably good considering the approximations made.

In Fig. 1(b), $\log(I)$ versus $\epsilon_g^{3/2}$ for several values of E_m is plotted for sample C. As E_m is increased, the slope of the data decreases, resulting in a roughly constant θ with an average value of $\bar{\theta} = 0.16 \pm 0.03$. Since θ depends only on the shape of the tunneling barrier and the effective mass, we expect it to be independent of E_m as is consistent with observation.

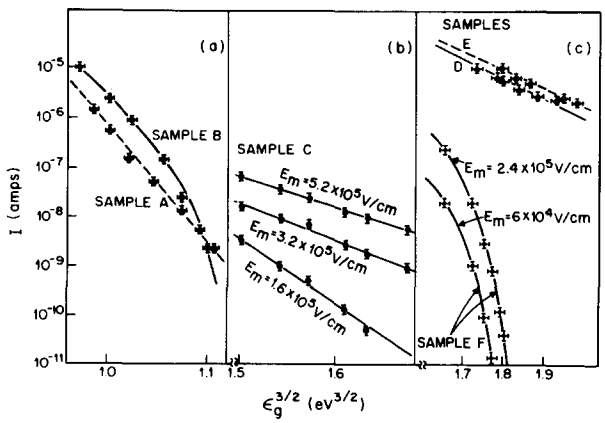

FIG. 1. Dependence of reverse-biased dark current, at fixed electric field on energy gap for several group III-V alloy diodes. (a) $In_xGa_{1-x}As_yP_{1-y}$ (b) InP at three values of maximum electric field, and (c) $Ga_xAl_{1-x}As$. Data for sample F given at $E_m = 2.4\times10^5$ V/cm and $E_m = 6.0\times10^4$ V/cm. Note changes in the horizontal scale.

Using the observed values of θ in Eq. (1), we find the magnitude of the calculated tunneling current is consistent with the currents measured for those samples exhibiting tunneling characteristics.

Note that the ratio $\epsilon_g^{3/2}/E_m$ given in Table I is largest for samples B and F. This implies a small tunneling probability compared with the other devices, perhaps accounting for deviations of the data from the form predicted. We find the data are consistent with tunneling when $\epsilon_g^{3/2}/E_m \leqslant 10^{-5}$ $eV^{3/2}$ cm/V, implying $E_m \gtrsim 10^5$ V/cm for our samples. This is an order of magnitude smaller than E_m required for observation of tunneling in silicon and germanium. However, m^*/m_0 is nearly an order of magnitude larger for silicon and germanium than for the III-V compounds studied, greatly reducing the tunneling probability. In addition, tunneling probability is smaller in indirect gap materials since phonon cooperation is necessary.

The data for sample B [Fig. 1(a)] depart from linearity only at the largest values of ϵ_g, implying that tunneling becomes increasingly dominant as ϵ_g decreases. A fit of the linear region of the data to Eq. (1) gives $\theta = 0.11 \pm 0.02$; a result consistent with values of θ obtained for the other samples.

To further test the tunneling model, the current-voltage characteristics of sample E (shown by the data points in the inset, Fig. 2) were used to obtain the dependence of current on $1/E_m$ at fixed ϵ_g, as shown in Fig. 2. The three sets of data were each taken at different temperatures, and therefore different $\epsilon_g(T)$. The data show considerable curvature at low electric fields, with the curvature more pronounced at higher temperatures. However, for $E_m \gtrsim 4\times10^5$ V/cm, the data are fit by the straight lines shown in the figure. This behavior indicates that tunneling becomes the dominant source of leakage with increasing field and decreasing temperature. Tunneling theory [Eq. (1)] predicts that the slopes κ of the straight lines follows $\kappa = \theta m_0^{1/2}\epsilon_g^{3/2}/(q\hbar)$. Indeed, we find the values of κ taken from Fig. 2 depend linearly on $\epsilon_g^{3/2}$. The slope of the best straight line fit to the κ-vs-$\epsilon_g^{3/2}$ data gives $\theta = 0.22 \pm 0.03$. This independent measurement of θ is consistent with θ obtained from the $\log(I)$-vs-$\epsilon_g^{3/2}$ measurements taken at constant electric field. When a similar field dependence analysis is applied to sample F, where $E_m < 2.4\times10^5$ V/cm, we find no region where $I \propto \exp(-\kappa/E_m)$. Thus, due to the large value of $\epsilon_g^{3/2}/E_m$, we find that tunneling is not a dominant contributor to the reverse-biased dark current in this device, consistent with the results shown in Fig. 1(c).

Deviations of the leakage current from Eq. (1) at low E_m and high temperature may be due to the dominance of other sources of leakage. Dark currents arising from thermally activated processes such as generation-recombination or thermally activated surface currents are expected to follow

$$I \propto \exp(-\Delta\epsilon/kT), \tag{3}$$

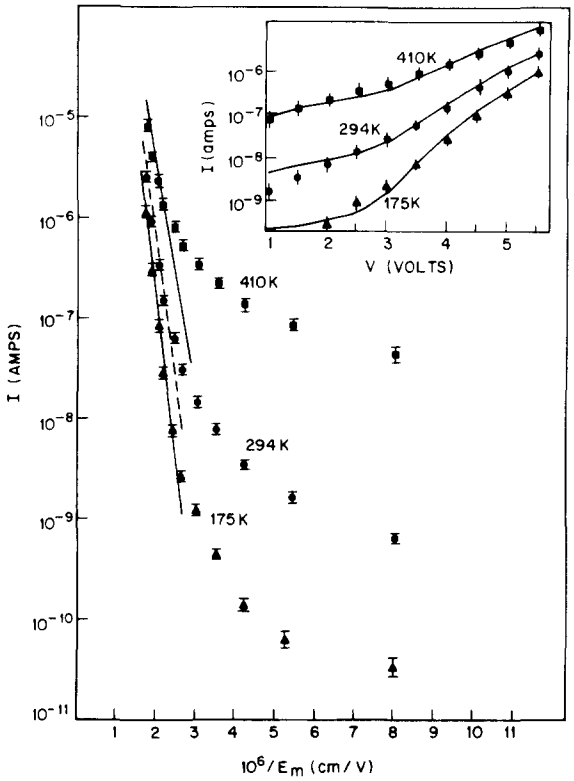

FIG. 2. Reverse-biased dark current dependence on maximum electric field for sample E at $T = 410$ K (squares), $T = 294$ K (dots), and $T = 175$ K (triangles). Straight line dependence in this plot indicates consistency with tunneling as given in Eq. (1). Inset: I-V characteristic at three temperatures. Solid lines indicate fit described in text.

where $\Delta\epsilon$ is the activation energy of the process. We have investigated whether the temperature dependence of our samples follows Eq. (3). For the low-doped samples, the leakage current does indeed appear to be a thermally activated process with a single activation energy over the entire temperature range investigated. In particular, for sample F $\Delta\epsilon = 0.27$ eV. This is the same activation energy obtained for the more highly doped sample E at low voltage (and therefore low electric field), where the current deviates from behavior consistent with tunneling [see Fig. (2)]. However, at high electric fields the dark-current behavior is consistent with tunneling but is found to be inconsistent with thermally activated processes as given by Eq. (3).

Thus, the reverse-biased leakage is dominated by tunneling at high fields (and therefore high voltage), and thermally activated currents dominate as the field is reduced. Fitting the measured data in Fig. 2 to the sum of a tunneling current [Eq. (1)] plus a thermal process with $\Delta\epsilon = 0.27$ eV gives the predicted voltage and temperature dependence shown by solid lines in the inset of Fig. 2. To fit the low-field data, we have assumed the thermally generated carrier lifetime is inversely proportional to the doping density. Also, a small contribution to the current due to a shunt resistence of $R_{\rm shunt} = 5\times10^9\ \Omega$ was included. Tunneling becomes dominant above ~ 3 V, where there is a sudden increase in the slope of the calculated leakage current. Since the above treatment is only intended as an approximation, we find the fit to be satisfactory.

In conclusion, we have presented evidence that a significant source of reverse-biased junction dark current in several III-V alloy semiconductors is due to tunneling, and further that the data are in good agreement with prediction for a band-to-band process. However, our measurements do not preclude the possibility of tunneling via traps in the band gap.[11] Indeed, trap-assisted tunneling has many of the same characteristics as the more fundamental band-to-band process. The tunneling current becomes dominant in these compounds at fields as low as 10^5 V/cm due to their small direct band gaps and small effective masses.

The presence of tunneling sets limits on the magnitude of the electric field allowable in the junction region above which the dark current becomes prohibitively large. In our devices, we find that tunneling is the dominant source of leakage over a wide range of applied voltages when the doping density is greater than 2×10^{16} cm^{-3}. The limitation set on electric field has significant impact on the capabilities and design considerations in several device applications.

We thank Yu-Ssu Chen for his suggestions and comments. We wish to thank V.G. Keramidas, W.A. Bonner, R.F. Leheny, and R.J. Nelson for supplying us with substrates and samples for measurements.

[1]K. Nishida, K. Taguchi, and Y. Matsumoto, Appl. Phys. Lett. **35**, 251 (1979).
[2]T.P. Lee, C.A. Burrus, and A.G. Dentai, IEEE J. Quant. Electron. **QE-15**, 30 (1979).
[3]C.A. Armiento, S.H. Groves, and C.E. Hurwitz, Appl. Phys. Lett. **35**, 333 (1979).
[4]Y. Takanashi and Y. Horikoshi, Jpn. J. Appl. Phys. **17**, 2065 (1978).
[5]F. Capasso, P.M. Petroff, W.A. Bonner, and S. Sumski (unpublished).
[6]G.E. Stillman and C.M. Wolfe, *Semiconductors and Semimetals*, edited by Willardson and Beers (Academic, New York, 1977), Vol. 12, p. 291.
[7]J.L. Moll, *Physics of Semiconductors* (McGraw-Hill, New York, 1964).
[8]Note added during review: We have found that for $In_{0.55}Ga_{0.45}As$, current is proportional to area, as predicted in Eq. (1). On reducing the diode mesa area one order of magnitude by etching, the dark current at $E_m = 2\times10^5$ V/cm was reduced from 28 to 3 μA. This behavior eliminates the surface as a significant source of dark current.
[9]Measurement of the junction doping profile via capacitance - voltage techniques for several devices indicates the number of ionized impurities, and therefore electric field, is temperature independent from 77 to 450 K. This supports the claim that constant applied voltage implies constant electric field.
[10]For InP, $m^*/m_0 \simeq 0.06$, see S.M. Sze, *Physics of Semiconductor Devices* (Wiley, New York, 1969); for $In_xGa_{1-x}As_yP_{1-y}$, $m^*/m_0 \simeq 0.04$, see H. Brendecke, H.L. Stormer, and R.J. Nelson, Appl. Phys. Lett. **35**, 772 (1979); and for $Ga_xAl_{1-x}As$, $m^*/m_0 \simeq 0.05$, see H. Temkin and V.G. Keramidas (unpublished). Here, m^* is the reduced effective mass of the electron in the valence and conduction bands.
[11]A.R. Riben and D.L. Feucht, Int. J. Electron. **20**, 583 (1966).